Circular Dichroism of Denatured Barstar Suggests Residual Structure[†,‡]

Bengt Nölting, Ralph Golbik, Andrés S. Soler-González, and Alan R. Fersht*

Cambridge University Chemical Laboratory and Cambridge Centre for Protein Engineering, MRC Centre, Hills Road, Cambridge CB2 2QH, U.K.

Received November 21, 1996; Revised Manuscript Received February 12, 1997[⊗]

ABSTRACT: The circular dichroism (CD) spectrum of the denatured state of barstar has been analyzed as a function of urea and temperature. The near- and far-UV CD spectra change very rapidly in magnitude and shape with increasing temperature, unlike those of native protein, suggesting the presence of residual structure that changes with denaturing conditions. The effect of mutations indicates that there is residual structure in $helix_1$ of the protein, consistent with NMR data. The changes in CD with conditions are consistent with the denatured state being a mixture of conformations of similar energy.

To assess the structural changes along the pathway of folding, it is important to know the structure, thermodynamics, and spectroscopic properties of the denatured states. In particular, it is crucial to know the differences in the residual structure between the different denatured states. Many important questions regarding denatured states of protein remain to be answered: What is the nature of the transitions between the different denatured states? Do the transitions involve cooperative melting of structure or gradual changes or no changes of structure at all? What is the energy landscape of a denatured protein? How might structures be funneled at the beginning of the folding reaction before reaching the first detectable transition state? How can the structural distribution of a denatured protein be resolved?

These questions are addressed by using circular dichroism (CD)[1] spectroscopic [Woody (1978), Vuilleumier et al. (1993), Snatzke (1994), and Duddeck (1995) and references therein] and equilibrium thermodynamic measurements of the cold-, heat-, and urea-denatured states and by analyzing the nature of the transitions between them. Despite CD having been used in a vast number of protein structure studies, the information content of the CD of denatured protein has been neglected. CD spectroscopy, which allows access to a wide range of temperature and time resolution (Kalnin & Kuwajima, 1995; Kuwajima et al., 1996), is seen here to be a sensitive probe for the denatured state of protein.

Spectroscopic differences between the cold-, heat-, and urea-denatured states of barstar (Hartley, 1988), the 10 kDa inhibitor of the ribonuclease barnase, are analyzed, and the structural and equilibrium thermodynamic implications are discussed. Barstar contains four α-helixes and a sheet with three strands (Figure 1). The native-like C40A/C82A/P27A barstar (pseudo-wild-type) (Nölting et al., 1995), used in this study has no cysteines that may give rise to cross links in the denatured state and only one proline residue. It is the first protein for which cold-unfolding was detected under physiologically relevant pH and ionic strength (Agashe & Udgaonkar, 1995; Nölting et al., 1995). Its folding pathway has been studied in detail and a Φ-value analysis (Fersht, 1993, 1995a) has been performed (Nölting et al., 1995, 1997). The structures along the folding pathway of barstar when refolding from the cold-denatured state in the microsecond to second time scale have been solved at the resolution of single residues (Nölting et al., 1997). Further, NMR evidence for the structure of the cold-denatured state of barstar (Wong et al., 1996) is available to complement the conclusions.

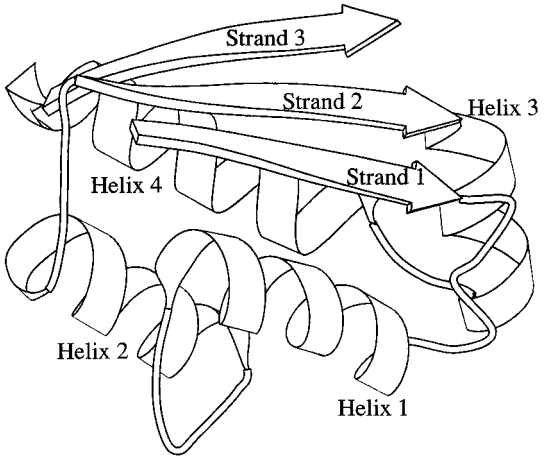

FIGURE 1: Structure of barstar [drawn with the program Molscript (Kraulis, 1991)]. The secondary structure of barstar is $Strand_1$(1−6), $Loop_1$(7−13), $Helix_1$(14−25), $Loop_2$(26−32), $Helix_2$(33−43), $Loop_3$(44−48), $Strand_2$(49−54), $Helix_3$(56−63), $Loop_4$(64−67), $Helix_4$(68−81), $Strand_3$(83−89).

MATERIALS AND METHODS

Protein Expression and Purification. The active pseudo-wild-type barstar that was used in this study is C40A/C82A/P27A barstar (Nölting et al., 1995). Site-directed mutagenesis of pseudo-wild-type barstar and its mutants, S14A, Q18G, A25G, Q58G, S59A, Q72G, and A77G, was performed using two sequential PCR steps (Ausubel et al., 1992) and inserting the mutated gene into the plasmid pML2bs (Nölting et al., 1995). Protein was expressed at 30 °C in the *Escherichia coli* strain BL21(DE3)(pLysE) (Novagen, Madison, WI) using 4 mM IPTG for induction. Site-directed mutagenesis of the pseudo-wild-type barstar mutants I5V and

[†] B.N. is supported by a European Union Human Capital and Mobility Fellowship and by a Medical Research Council Fellowship.

[‡] Dedicated to the memory of Günther Snatzke (1928−1992).

[⊗] Abstract published in *Advance ACS Abstracts,* July 15, 1997.

[1] Abbreviations: CD, circular dichroism; pseudo-wild-type barstar, C40A/C82A/P27A barstar; IPTG, isopropyl 1-thio-β-galactoside; Tris-HCl, tris(hydroxymethyl)aminomethane hydrochloride; UV, ultraviolet.

S0006-2960(96)02879-6 CCC: $14.00

L34V was performed as described (Nölting et al., 1995). All mutants display significant activity in an assay with barnase (Hartley & Smeaton, 1973). Wild-type barnase was expressed and purified as described (Serrano et al., 1990). Barnase and barstar concentrations were determined using an extinction coefficient at 280 nm of 27 400 L mol^{-1} cm^{-1} (Vuilleumier et al., 1993) and 22 690 L mol^{-1} cm^{-1} (Schreiber & Fersht, 1993; Lubienski et al., 1994), respectively.

CD Studies of the Native State and the Transition to the Denatured State. CD spectra were obtained using a Jasco (Easton, MD) Model J-720 spectrometer with a spectral resolution of 2 nm. It was interfaced with a computer-controlled Neslab (Newington, NH) RTE-111 water bath. CD calibration was performed using (1S)-(+)-10-camphorsulfonic acid (Aldrich) with a molar extinction coefficient of 34.5 M^{-1} cm^{-1} at 285 nm and a molar ellipticity of 2.36 M^{-1} cm^{-1} at 290.5 nm. For measurements below 5 °C, the sample was preequilibrated at the desired temperatures for 1 h. In urea-induced unfolding experiments of pseudo-wild-type barstar (Figure 4), the measured mean residual ellipticity at 222 nm, $S = \Delta\epsilon_{R,222}$, of the mixture of native and denatured states as a function of the denaturant concentration, [D], was fitted to

$$S = [\alpha_N + (\alpha_D + \beta_D[D])K]/[1 + K] \quad (1)$$

$$K = \exp\{m([D] - [D]_{50\%})/(RT)\} \quad (2)$$

where α_N is the mean residual ellipticity of the native state, −5.2 L mol^{-1} cm^{-1} at 222 nm; α_D and β_D define a linear approximation for the mean residual ellipticity of the denatured state; $[D]_{50\%}$ is the concentration of denaturant at the midpoint of the transition; $m \equiv -\partial(\Delta G_{D\text{-}N})/\partial[\text{urea}] =$ 1.25 kcal L mol^{-2} (1 kcal = 4.18 kJ), where $\Delta G_{D\text{-}N}$ is the free energy of denaturation (Nölting et al., 1995); and R and T are the universal gas constant and absolute temperature, respectively. The quality of the linear approximation for the signal of the denatured state was tested at −4 and 25 °C by calculating the mean residual ellipticity of the denatured state, $\Delta\epsilon_{R,222}(D) = (S[1 + K] - \alpha_N)/K$, by using the measured S and the result of the fit for α_N, m, and $[D]_{50\%}$ (Figure 4, closed circles and squares). The relative errors of S and α_N over the range of denaturant concentration are both ±0.05 L mol^{-1} cm^{-1}. Peptides of barstar comprising residues 11−29 (labeled $helix_1$ since it contains all residues of $helix_1$ in native barstar) and 33−44 ($helix_2$) (Nölting et al., 1997) were used with the same buffer and residual concentration as barstar. The aromatic residues are Tyr29 in the $helix_1$ peptide and Trp38 and Trp44 in the $helix_2$ peptide.

Temperature scans in 3 M urea were done with a heating rate of 20 °C h^{-1} below 25 °C and 50 °C h^{-1} above 25 °C. The absolute error in temperature is ±1.5 °C. The absolute error of the CD signal, resulting from the error in the determination of the protein concentration and errors in the CD calibration, is estimated to be ±6% at 25 °C. The reversibility of thermal unfolding in 3 M urea was >90%.

CD Studies of the Denatured State. The heating rate for temperature scans under unfolding conditions was 50 °C h^{-1}. The reversibility of the temperature-induced changes in the denatured state was better than 99.5%, as judged by heating of a sample in 7 M urea at 20 °C h^{-1} from 1 to 95 °C, then cooling down to 1 °C, and heating again to 95 °C at 60 °C h^{-1}. CD measurements shown in each diagram were done with the same sample cell and batch of protein. The relative error for scans in Figure 6A,D is ±0.03 L mol^{-1} cm^{-1} ± 2% $\Delta\epsilon_{R,230}$. The relative error of $\Delta\epsilon_R$ for the other scans in Figure 6B,C is ±0.01 L mol^{-1} cm^{-1} ± 1% $\Delta\epsilon_{R,230}$ as judged by the reproducibility. No differences were noticed for different temperature scan rates above 20 °C. The systematic error of $\Delta\epsilon_{R,230}$ due to kinetic effects is up to −0.01 L mol^{-1} cm^{-1} between 10 and 20 °C and up to −0.02 L mol^{-1} cm^{-1} between 2 and 10 °C. Temperature scans were started at a 5 °C lower temperature than shown in the figures. The relative error in temperature for curves in one diagram is less than ±0.3 °C. Poly(ethylene glycol) with an average molecular weight of 8000 (PEG 8000) was from Sigma (St. Louis, MO). Data were processed with Kaleidagraph (Synergy Software, Reading, PA).

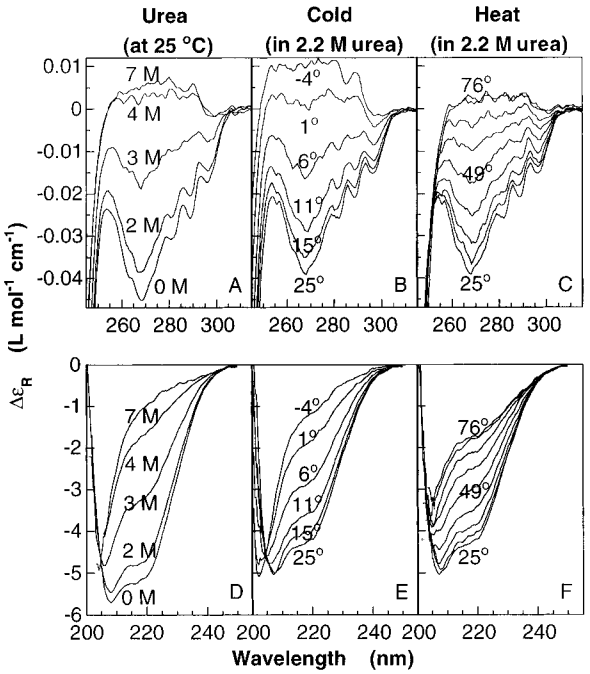

FIGURE 2: Equilibrium unfolding of C40A/C82A/P27A (pseudo-wild-type) barstar monitored by mean residual ellipticity, $\Delta\epsilon_R$. Conditions for near-UV CD were 50 μM protein in 50 mM Tris-HCl buffer at pH 8 with 0.1 M KCl, and the path length was 1 cm. (A) Urea-induced unfolding at 25 °C. Values of [urea] are 0, 2, 3, 4, and 7 M. (B) Cold-induced unfolding in 2.2 M urea. Temperatures are 25, 15, 11, 6, 1, and −4 °C. (C) Heat-induced unfolding in 2.2 M urea. Temperatures are 25, 35, 39, 44, 49, 54, 58, 67, and 76 °C. Conditions for far-UV CD were 60 μM protein in 50 mM Tris-HCl buffer at pH 8 with 0.1 M KCl, and the path length was 0.02 cm. (D) Urea-induced unfolding at 25 °C. Values of [urea] are 0, 2, 3, 4, and 7 M. (E) Cold-induced unfolding in 2.2 M urea. Temperatures are 25, 15, 11, 6, 1, and −4 °C. (F) Heat-induced unfolding in 2.2 M urea. Temperatures are 25, 35, 39, 44, 49, 54, 58, 67, and 76 °C.

Table 1. The error for $\Delta\epsilon_{R,222}$ of the denatured mutants relative to pseudo-wild-type is ± 0.03 L mol^{-1} cm^{-1}. The change of free energy of unfolding, $\Delta\Delta G_{D\text{-}N}$, upon mutation was measured as described (Nölting et al., 1995). The surface accessibility was calculated for a Connolly surface with 1.4 Å radius using WHATIF.

RESULTS

Near- and Far-UV CD Spectra. Denaturation of barstar by urea, cold and heat (Figure 2) causes a weakening of the near-UV CD signal at 260−290 nm and a change of sign,

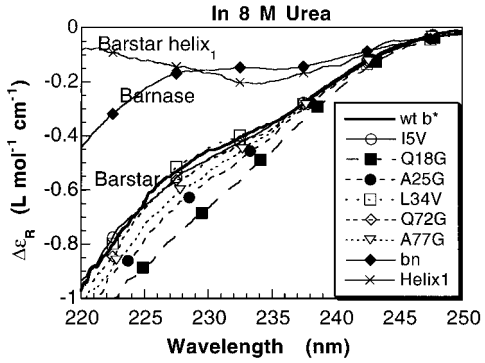

FIGURE 3: Spectra of the mean residual ellipticity, $\Delta\epsilon_R$, of a peptide of barstar comprising residues 11−29 (helix$_1$) and of the urea-denatured states of barnase, C40A/C82A/P27A barstar, and its mutants: I5V, Q18G, A25G, L34V, Q72G, and A77G. Different symbols are used for clarity and do not reflect the number of measured points. Conditions were 5 μM protein or 10 μM peptide in 50 mM potassium phosphate buffer with 8 M urea at pH 8 with 0.1 M KCl at 25 °C and a path length of 1 cm.

because of a loss of chiral environment of the aromatic side chains (Woody, 1978, 1994; Vuilleumier et al., 1993) Trp 38, 44, and 53; Tyr 29, 30, and 47; and Phe 56 and 74 (Hartley, 1988). The most red-shifted features at 290−300 nm arise from deeply buried side chains in the native structure (Woody, 1994) and accordingly disappear on denaturation. The random coil-like shape and magnitude of the far-UV CD spectra suggest a significant loss of secondary structure in all three denatured states (Figure 2D−F). While the CD signal of the denatured state at 260−290 nm and at 200−210 nm weakens, at 220−230 nm it strengthens dramatically upon temperature rise (Figure 2).

Effects of Mutations on the CD in the Denatured State. The far-UV CD of denatured barstar is significantly more negative than that of barnase or peptides of barstar comprising residues 11−29 (helix$_1$) (Figure 3) and 33−44 (helix$_2$) (not shown). The nine pseudo-wild-type barstar mutants measured affect interactions: in strand$_1$ (I5V); in helix$_1$ (S14A, Q18G, and A25G); in helix$_2$ (L34V); in helix$_3$ (Q58G and S59A); and in helix$_4$ (Q72G, A77G). The mutants I5V, L34V, S59A, and A77G affect also significantly interactions in the hydrophobic core (Table 1). The mutations located in helix$_1$ are found to display the largest difference of CD relative to pseudo-wild-type barstar (Figure 3). These observations coincide with the finding of residual structure in helix$_1$ of denatured barstar (Wong et al., 1996) but there is no NMR indication for nonrandomly oriented conformations in the helix$_1$ and helix$_2$ peptides (J. L. Neira, A. S. Soler-González, and A. R. Fersht, unpublished data).

Urea-Induced Transitions in the Denatured State. Pseudo-wild-type barstar was titrated with urea at −4, 10 (not shown), and 25 °C in order to study the nature of transitions in the denatured state (Figure 4). The change of the mean residual ellipticity at 222 nm, $\Delta\epsilon_{R,222}$ (liters per mole per centimeter), with [urea], $\partial(\Delta\epsilon_{R,222})/\partial$[urea], of the denatured state is found to be only 0.09 L^2 mol^{-2} cm^{-1}, and no cooperative transitions or nonlinearity of the signal as a function of [urea] (Tanford, 1970) were detected within experimental error (Figure 4). Virtually the same urea increments were found for the helix$_1$ and helix$_2$ peptides, which display significantly weaker $\Delta\epsilon_{R,222}$ and for which no residual structure was detected in NMR (Nölting et al., 1997). For comparison, at the midpoint of the transition from the native to the denatured state of barstar, $\partial(\Delta\epsilon_{R,222})/\partial$[urea] = 2.1 L^2 mol^{-2} cm^{-1}.

Thermal Scans. Figure 5 shows the thermal denaturation of pseudo-wild-type barstar in 3 M urea. The major reason for cold denaturation is thought to be the decrease of the hydrophobic effect with decreasing temperature (Privalov, 1990). Thus, the low ratio of electrostatic to hydrophobic contributions to the stability of barstar, which has a net charge of −5, may explain the early onset of cold denaturation.

$\Delta\epsilon_{R,222}$ of the native state in the absence of denaturants at 25 °C is (−5.2 ± 0.3) L mol^{-1} cm^{-1} (Figure 5, 0 M). The change of the observed signal when [urea] is increased from 0 to 1 M results mainly from a slight degree of unfolding since the free energy of unfolding, $\Delta G_{D\text{-}N}$, at 10 °C changes from 3 to 1.8 kcal mol^{-1}, corresponding to a change from 0.6% to 4% population of the denatured state. The change of $|\Delta\epsilon_{R,222}|$ of the native state with [urea], caused by solvent effects on surface-exposed peptide chromophores, is <0.05 L^2 mol^{-2} cm^{-1}, corresponding to a relative change of <1% L mol^{-1}. The decrease with increasing temperature of $|\Delta\epsilon_{R,222}|$ of the native state at 25 °C in the absence of urea is very small, ≤0.01 L mol^{-1} cm^{-1} K^{-1}, corresponding to a relative change of ≤0.2% K^{-1}. The slight curvature in 0 and 1 M urea (Figure 5) is mainly caused by a change of the population of the native state, as estimated from the free energy of unfolding, $\Delta G_{D\text{-}N}$, under different conditions. For example, $\Delta G_{D\text{-}N}$ in 1 M urea decreases from about 2.0 to 1.5 kcal mol^{-1} upon cooling from 25 to 4 °C, corresponding to a depopulation of the native state by a further 3%, which accounts for a change of $\Delta\epsilon_{R,222}$ by about 0.15 L mol^{-1} cm^{-1}. The very small temperature dependence of the native state is expected since the chiral environment of the peptide chromophores in the unique native conformation should change only slightly with temperature. Very small temperature-induced relative changes of $|\Delta\epsilon_{R,222}|$ have been reported also for native tropomyosin, 0.25−0.4% K^{-1}, and paramyosin, 0.17−0.22% K^{-1} [Holtzer and Holtzer (1992) and references therein].

Transition between Cold- and Heat-Denatured State. The remarkably large and slightly nonlinear changes of the CD signal in the transition between the cold- and heat-denatured state do not appear to fit the sigmoidal shape of cooperative transitions (Figure 5). $\Delta\epsilon_{R,222}$ (liters per mole per centimeter) of the denatured state of pseudo-wild-type barstar as a function of temperature, Θ(°C), from 5 to 95 °C fits to a single-exponential function:

$$\Delta\epsilon_{R,222}(\Theta) = A + B\exp(-C\Theta) \qquad (3)$$

with $A = -2.16 \pm 0.03$, $B = 2.17 \pm 0.02$, and $C = 0.0157 \pm 0.0004$ [standard deviations of the fit are as indicated; A and B are in units of liters per mole per centimeter and C is in units of (degrees Celsius)$^{-1}$], respectively, in 8 M urea. Dramatic temperature-induced changes of the CD of denatured barstar are observed at essentially all wavelengths between 200 and 300 nm, with the exception of around 210 nm where the sign of the temperature increment of CD changes (Figure 2).

CD Temperature Scans of the Denatured State under Different Conditions. The mean residual ellipticity of denatured barstar at 230 nm, $\Delta\epsilon_{R,230}$, displays qualitatively similar dramatic temperature changes like $\Delta\epsilon_{R,222}$ but is easier

Table 1: Structure, Change of Free Energy of Unfolding upon Mutation, and Mean Residual Ellipticity of Mutants of Pseudo-Wild-Type Barstar

barstar mutant	position of mutation	surface accessibility of residue in folded wild-type barstar (Å^2)	$\Delta\Delta G_{D\text{-}N}$ (kcal mol^{-1})	$\Delta\epsilon$R,222, 8 M urea, 25 °C (L mol^{-1} cm^{-1})
pseudo-wt				−0.85
15V	strand 1	0	1.0	−0.84
S14A	helix 1	61	0.5	−0.93
Q18G	helix 1	84	1.3	−1.03
A25G	helix 1	68	1.3	−0.98
L34V	helix 2	72	1.1	−0.83
Q58G	helix 3	71	1.6	−0.86
S59A	helix 3	0	1.3	−0.86
Q72G	helix 4	108	1.2	−0.87
A77G	helix 4	1	2.0	−0.92

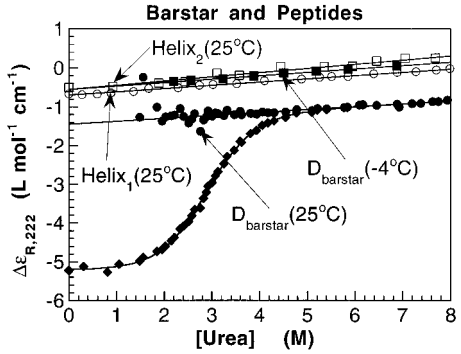

FIGURE 4: Urea-induced transitions in the denatured state of C40A/C82A/P27A barstar at −4 °C (■) and 25 °C (●) monitored by the mean residual ellipticity, $\Delta\epsilon_{R,222}$, of the denatured state at 222 nm. $\Delta\epsilon_{R,222}$ of the denatured state was calculated from unfolding curves (shown with ◆ for 25 °C) (see Materials and Methods). For example, in 1 M urea at 25 °C, the population of the denatured state is about 4%. For comparison, the urea-induced changes in peptides of barstar comprising residues 11−29 (helix$_1$) and 33−44 (helix$_2$) are shown. Conditions were 60 μM protein or peptide in 50 mM Tris-HCl buffer at pH 8 with 0.1 M KCl, and the path length was 0.1 cm.

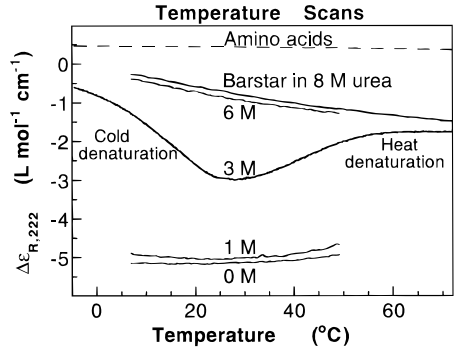

FIGURE 5: Temperature dependence of the mean residual ellipticity at 222 nm, $\Delta\epsilon_{R,222}$, of C40A/C82A/P27A barstar at different [urea], as indicated. Conditions were 50 μM protein in 50 mM potassium phosphate buffer at pH 8 with 0.1 M KCl, and the path length was 0.1 cm. For comparison $\Delta\epsilon_{R,222} = 0.462 - (3.52 \times 10^{-4})\theta - (1.34 \times 10^{-5})\theta^2$, where θ is the temperature (degrees Celsius) of a mixture of amino acids that corresponds to the composition of barstar, is shown with a dashed line.

to record at high [urea] since urea absorbs in the UV (Figure 6A). The scans of the mutants I5V and L34V differ only slightly from those of pseudo-wild-type barstar. In contrast, the scan of barnase displays a significantly different amplitude and curvature, suggesting that the CD of the denatured state depends on the particular protein but that the convex shape is not unique for barstar and may be a general feature of denatured proteins.

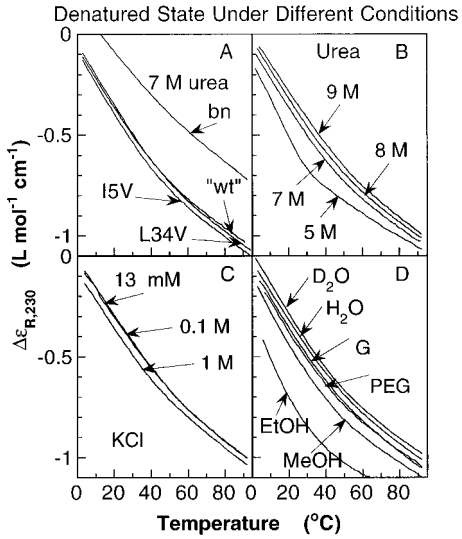

FIGURE 6: Changes of the mean residual ellipticity at 230 nm, $\Delta\epsilon_{R,230}$, of the denatured state of C40A/C82A/P27A barstar under the influence of various factors. Conditions were 6 μM protein in 50 mM potassium phosphate buffer at pH 8, and the path length was 1 cm. [KCl] is 0.1 M unless stated otherwise. (A) Effect of mutation. Pseudo-wild-type (wt) and mutants (I5V and L34V) in 7 M urea. For comparison, barnase (bn) is shown. (B) Urea effect. [Urea] is 5, 7, 8, and 9 M. (C) Salt effect. The protein is in 9 M urea and 13 mM KCl (13 mM), in 9 M urea and 0.1 M KCl (0.1 M), in 9 M urea and 1 M KCl (1 M), in 7 M urea and 1 M KCl (1 M/7), and in 5 M urea and 0.1 M KCl (0.1 M/5). (D) Solvent effect. The protein is in 8 M urea and buffer (H_2O), in 8 M urea and 8% glycerol (G), in 7.1 M urea and 10% poly(ethylene glycol) (PEG), in 7 M urea and 20% methanol (MeOH), in 7 M urea and 20% ethanol (EtOH), and in 8 M urea and 72% D_2O (D_2O). The percentages are in volume of cosolvent per total volume of mixture. [Urea] refers to the amount of urea per total volume of mixture, including the solvent-inaccessible volume.

The curves of $\Delta\epsilon_{R,230}$ at different [urea] (Figure 6B) are parallel, within experimental error, and, similar to $\Delta\epsilon_{R,222}$ (Figure 5), the dependence on [urea] is small. The difference of the curvature from that of the transition to the native state becomes obvious when [urea] is lowered to 5 M, where the native state is slightly populated (Figure 6B).

Despite the large increase in stability, 2.4 kcal mol^{-1}, of the native protein on increasing KCl from 0.1 to 1 M at 5−7 M urea (Figure 6C), $\Delta\epsilon_{R,230}$ of the denatured state increases only slightly upon addition of salt (Figure 6C).

The CD of cold- as well of heat-denatured state displays a small but significant isotope effect on replacing H_2O with D_2O (Figure 6D). The denatured state consists of a large number of rapidly interconverting conformations with similar free energy and so involves rearrangement of solvent.

Pseudo-wild-type barstar is 0.7 kcal mol^{-1} more stable in D_2O than H_2O at 25 °C, compared with 1.4 kcal mol^{-1} for barnase (Perrett, 1995).

Organic solvent mixtures were used for comparison with the urea−water mixture. High molecular weight poly(ethylene glycol) (PEG) is considered to exhibit properties close to that of an ideal osmolyte up to high concentrations (Castellino & Barker, 1968; Parsegian et al., 1986; Jung et al., 1996), and decreases the water activity without interacting specifically with protein. In contrast to the effect of urea, which is thought to form hydrogen bonds with the amide group of proteins, the presence of PEG, glycerol, methanol, and ethanol causes an increase of the absolute CD signal (Figure 6D). The relative effects are about 1:1:4 for glycerol, methanol, and ethanol at the same concentration, indicating a positive correlation with the hydrogen-bonding ability. No strong correlation is indicated with the dielectric constants, which are 79, 43, 33, and 24 for water, glycerol, methanol, and ethanol, respectively, at 25 °C (Bruno & Svoronos, 1989). There is no strong correlation with viscosity. The microscopic viscosity is largest for glycerol mixtures. PEG causes a large increase in the macroscopic viscosity. The effects of major changes in solvent are small compared with that of changes in temperature (Figure 6).

The changes of $\Delta\epsilon_{R,230}$ (liters per mole per centimeter) of the denatured state of barstar in 50 mM potassium phosphate buffer with 7 M urea and 0.1 M KCl at 25 °C upon change of conditions (in parentheses) are −0.13 (+10 °C), +0.05 (+1 M urea), −0.06 (+1 M KCl), +0.03 (in 72% D_2O), and −0.01 (+8% PEG).

DISCUSSION

Thermal Transitions between the Denatured States. Little, if any, precise data for the temperature dependence of the CD signals of denatured states of protein are available in the literature and the information content is usually neglected. Precise measurements of pseudo-wild-type barstar (Figures 5 and 6) show a significant, slightly nonlinear change of the CD signal of the denatured state with *T*. The large temperature-induced changes are highly reversible, do not significantly depend on the temperature scan rate between 20 and 60 °C h^{-1} above 20 °C, do not significantly change with the protein concentration between 6 and 60 μM, and are not unique to barstar, since barnase also shows qualitatively similar effects (Figure 6A). In contrast to the changes connected with the transition of most native globular proteins from the native to the denatured state, the CD of the denatured state of barstar around 222 nm becomes more negative upon heating (Figure 5). The sign of the CD changes matches that for temperature-induced phase transitions of synthetic poly-L-proline II, poly-L-glutamic acid, poly-L-lysine, and poly-L-aspartic acid (Tiffany & Krimm, 1968, 1969, 1972), which display a positive CD signal at 210−220 nm at room temperature, however.

The mean residual ellipticity at 230 nm, $\Delta\epsilon_{R,230}$ (liters per mole per centimeter), which is easier to measure than at 222 nm in high [urea], as function of temperature, Θ (degrees Celsius) of the denatured state of barnase in 8 M urea fits to $\Delta\epsilon_{R,230}(\Theta) = -1.65 + 1.80 \exp(-0.0072\Theta)$, and that of pseudo-wild-type barstar fits to $\Delta\epsilon_{R,230}(\Theta) = -1.52 + 1.52 \exp(-0.0119\Theta)$. The large temperature-induced changes cannot be explained by a contribution of the native state to the mean residue ellipticity, which is only -3×10^{-4} L mol^{-1} cm^{-1} in 7 M urea at 25 °C, calculated from its measured free energy of folding.

Temperature-Induced Changes of CD Reflect Changes in Structure of the Denatured State. The evidence for the structural significance of the CD changes of denatured barstar with temperature is as follows: (1) In contrast to the denatured state, the native state at 20−40 °C displays 3−10 times smaller temperature-induced changes of opposite sign (Figure 5). (2) Many rigid molecules, such as amino acids (Figure 5, dashed line), display comparably small CD changes. (3) The CD changes differ dramatically in magnitude between different denatured proteins and peptides. (4) The large far-UV CD and the effect of mutants coincides with the observation of residual structure is $helix_1$ by NMR (Wong et al., 1996). (5) The CD changes of denatured barstar occur in essentially the whole wavelength region between 200 and 300 nm, with the exception of an isodichroic point at about 210 nm (Figure 2). (6) The sign of these CD changes around 205 nm and in the 220−230 nm region matches that for temperature-induced phase transitions of synthetic polypeptides (Tiffany & Krimm, 1972).

These observations are inconsistent with the assumption of only an intrinsic temperature dependence of the CD chromophores and together suggest that the main contributions to the temperature dependence of the CD arise from changes in the protein conformation. This conclusion is supported by a study on myosin [Holtzer and Holtzer (1992) and references therein], where temperature changes of $|\Delta\epsilon_{R,222}|$ in the native state as little as 0.2−0.4% K^{-1} have been attributed to changes in helix content.

Analysis of the Temperature Dependence of the CD. The absorption of a photon by a chromophore causes a movement in the electron distribution of the molecule, which may be described as a transition dipole (Snatzke, 1994; Woody, 1994). Transition dipoles are sensitive to their environment. Important factors that change with temperature are average orientation of the chromophores in the molecule, intramolecular collisions, collisions of the chromophore with solvent, average dielectric constant of the environment, and hydrogen bonding.

Each thermodynamic state of a protein has a conformational distribution, which is narrow for rigid states, such as the native state, and wide for flexible states, such as the denatured state. Higher temperature causes a larger occupancy of higher energy conformations, which may have different orientations of their transition dipoles, given by Boltzmann's statistics. The average value of thermal energy is about 0.6 kcal mol^{-1} at 28 °C and about 37% of the molecules possess an energy above average. The temperature increment of the average thermal energy is very small, roughly 2 cal mol^{-1} K^{-1}. That is why for rigid molecules usually the temperature increment of the absolute CD is very small. For denatured protein, however, these small energy changes cannot necessarily be neglected. Denatured protein at higher temperature may fill a larger conformational space due to its higher thermal energy than at low temperature. According to this interpretation, a large temperature increment of the absolute CD signal, similar to that observed for the denatured state, suggests the changes in population of states with similar free energy but significantly different conformations, i.e., a shallow energy landscape (Frauenfelder et al., 1991; Su et al., 1996; Wolynes et al., 1996). This

indication is further supported by the following: (1) Cooperative transitions that may be observed even in proteins of only 1−3 kcal mol^{-1} stability (Burova et al., 1995; Nölting et al., 1995) are absent in temperature scans (Figure 6). (2) The rate constant of conformational exchange of cold-denatured barstar is $>10^3$ s^{-1} (Wong et al., 1996). (3) Temperature changes of CD of many rigid molecules, such as the native state and amino acids in solution, are small.

Further, the shape of the energy landscape of denatured protein at low energies, i.e., less than about 2 kcal mol^{-1}, may change with temperature, for example, due to the increase of the hydrophobic effect with temperature. Changes in the average dielectric constant of the environment and in hydrogen bonding cause spectral line shifts. Protein−solvent and intramolecular collisions cause line broadening. The solvation of a protein is thought to decrease with increasing temperature (Makhatadze & Privalov, 1993; Privalov & Makhatadze, 1993). Furthermore, the nonhomogeneity of the occupancy of the solvent shell around the peptide chromophores may change with temperature. However, the relatively small effects of urea, glycerol, and methanol (Figure 6) and the very small temperature-induced changes of CD for the native state (Figure 5) and many rigid molecules suggest only a small contribution of changes in solvation to the temperature dependence of $\Delta\epsilon_{R,230}$ of pseudo-wild-type barstar in urea−water mixtures. The very small temperature increment of the CD for the native state indicates only a small contribution of intramolecular collision broadening.

Small but significant temperature increments of absolute CD are observed also in the helix$_1$ and helix$_2$ peptides of barstar, for which no residual structure was detected within the resolution of NMR (Nölting et al., 1997), suggesting a significantly higher sensitivity of CD. For example, the temperature increment of $|\Delta\epsilon_{R,222}|$ of the helix$_2$ peptide at 25 °C in 8 M urea is about half that of denatured barstar (not shown). Thus there are also significant changes in the structure of peptides with temperature. For detection of residual structure in NMR, an internal standard was used for the signal of the so-called random-coil conformation. This standard shifts with changes of temperature or [denaturant], which makes it difficult to detect small changes of structure contents (Wong et al., 1996).

Nature of the Residual Structure in the Denatured States. The large negative far-UV CD signal with a shoulder around 220 nm of denatured barstar (Figures 2D−F and 3) indicates a significant amount of not randomly orientated structure (Jasanoff & Fersht, 1994). $\Delta\epsilon_{R,222}$ of denatured barstar is roughly twice as large as that of barnase (Figure 3). Small CD signals cannot easily be attributed to a specific type of residual structure. However, (ϕ, Ψ) angles that are typically found in α-helices, β-sheets, and β-turns account for negative CD contributions around 220−230 nm (Woody, 1994). The so-called random-coil conformation, which may cause weak positive or negative CD contributions around 200−230 nm, displays a significant occupancy of (ϕ, Ψ) angles in the helical space (Serrano, 1995; Smith et al., 1996). A large negative CD signal of α-helical structure arises only if residues with (ϕ, Ψ) angles in the helical space have neighbors also with helical structure. Further, aromatic chromophores may account for positive and negative contributions to the CD signal in the 215−230 nm region (Vuilleumier et al., 1993; Woody, 1994).

The far-UV CD, $\Delta\epsilon_R$, displays a surprising sensitivity to the point mutations Q18G and A25G, located in helix$_1$ (Figure 3, Table 1). Similar to the changes upon increased temperature, both mutations cause an increase of the negative far-UV CD signal. In contrast, the chemically similar mutants Q72G and A77G, located in helix$_4$, and Q58G, located in helix$_3$, display little if any difference relative to pseudo-wild-type. Similarly, $\Delta\epsilon_{R,230}$ of S14A in helix$_1$ is more negative than that of S59A in helix$_3$. The direction of CD change is the same as found for temperature increase. The increased $|\Delta\epsilon_R|$ of Q18G may be due to the formation of turns, which may give rise to a negative signal around 225 nm. Another possibility is a more random distribution of aromatic side chains due to loss of residual structure upon mutation, which can cause also a more negative signal in the 215−230 nm region. The sources of such a contribution are unlikely to be Trp38 or Phe56, however, since the mutants W38F and F56A cause positive changes of $\Delta\epsilon_{R,222}$ (not shown). In both cases, a tendency to form residual structure in helix$_1$ is suggested: destabilizing mutations at positions that are completely randomly orientated should not cause a significant CD change beyond their intrinsic contributions. It should be noted that, from the observation of no CD change upon mutation, one cannot conclude the absence of residual structure, since the modified structure may have the same signal. Furthermore, in cases of significant changes, one has to check if these are not caused by intrinsic, chemical changes of the CD chromophores. Thus, a set of mutants may provide a probability for the occurrence of residual structure.

These indications are consistent with an NMR investigation of the cold-denatured state of barstar, revealing residual structure in helix$_1$ and helix$_2$ and strand$_2$ (Wong et al., 1996). β-turn-like conformations have been detected in the denatured states of barnase at the position of a β-hairpin of the native state (Arcus et al., 1995; Neira & Fersht, 1996).

Residual Structure Does Not Involve Significant Surface Burial. The absence of cooperative transitions in CD scans suggests that no significant permanent breaking or forming of bonds occurs upon the transitions between the three denatured states. The small (only 4% that of the unfolding transition of barstar at its midpoint) and similar urea increment of $\Delta\epsilon_{R,222}$ for denatured barstar and two of its peptides with significantly lower degrees of residual structure (Figure 4) indicates a very low degree of surface burial caused by the residual structure of denatured barstar and a similar solvent exposure of denatured conformations under folding conditions relative to that under strongly unfolding conditions. The significant temperature increment of the absolute CD signal (Figures 5 and 6) may be explained by an increasing population of higher energy conformations of the denatured protein with temperature and slight changes in the shape of the energy landscape with temperature, possibly connected with changes in the overall expansion of the molecule (Konno et al., 1995).

Hydration and Conformational Entropy of the Denatured State. The hydrational contributions per residue to the free energy, enthalpy, and entropy changes upon transition to the ideally unfolded state of four small globular proteins at 25 °C have been estimated to be roughly −10 kcal mol^{-1}, −20 kcal mol^{-1}, and −20 cal mol^{-1} K^{-1}, respectively (Makhatadze & Privalov, 1993; Privalov & Makhatadze, 1993). The conformational contributions have nearly the same value with

opposite sign, and the observed values at room temperature are typically 3 orders of magnitude smaller. The changes in the observed values on reducing the water activity are comparably small (Jiang et al., 1996). For example, the addition of 8% PEG is found to increase the free energy of unfolding of barstar by only 1.0 ± 0.2 kcal mol^{-1}. This suggests that the denatured state, according to the principle of Le Chatelier, escapes the osmotic pressure by readjusting the balance between hydrational and conformational contributions to free energy, and enthalpy and entropy as well. Thus, when water activity was reduced by about 8%, the magnitude of the conformational entropy of the denatured state of barstar decreases by roughly 8%. The modest effect of PEG on $\Delta\epsilon_{R,230}$ suggest that the CD is not very sensitive to the number of conformations of the denatured state (Figure 6D).

Implications for Protein Folding Studies and Models of the Folding Reaction. Denatured states of protein may contain a significant amount of structure (Pfeil, 1988; Dill & Shortle, 1991; Neri et al., 1992; Pfeil et al., 1993; Arcus et al., 1994, 1995; Freund et al., 1996). Despite the low stability of the residual structure of barstar, it melts only gradually when [urea] is increased because only very little change in buried surface is involved. The interpretation of the temperature increment of the absolute CD signal is consistent with a shallow energy landscape of denatured protein allowing large conformational changes with little energy change initially in the folding reaction (Wolynes et al., 1995). Initially in the folding reaction, the relative changes of CD may be larger than the relative changes of energy. This prediction matches the observations for the microsecond intermediate of barstar, which displays a relatively larger amount of structure formation, 40% as judged by far-UV CD, than amount of energy gain, 20% of the native state (Nölting et al., 1997).

REFERENCES

Agashe, V. R., & Udgaonkar, J. B. (1995) *Biochemistry 34*, 3286−3299.

Arcus, V. L., Vuilleumier, S., Freund, S. M. V., Bycroft, M., & Fersht, A. R. (1994) *Proc. Natl. Acad. Sci. U.S.A. 91*, 9412−9416.

Arcus, V. L., Vuilleumier, S., Freund, S. M. V., Bycroft, M., & Fersht, A. R. (1995) *J. Mol. Biol. 254*, 305−321.

Ausubel, F. M., Brent, R., Kingston, R. E., Moore, D. D., Seidman, J. G., Smith, J. A., & Struhl, K., Eds. (1992) *Short Protocols in Molecular Biology*, pp 8.23−8.25, Wiley, New York.

Bruno, T. J., & Svoronos, P. D. N. (1989) *CRC Handbook of Basic Tables for Chemical Analysis*, p 212, CRC Press, Boca Raton, FL.

Burova, T. V., Bernhardt, R., & Pfeil, W. (1995) *Protein Sci. 4*, 909−916.

Castellino, F. J., & Barker, R. (1968) *Biochemistry 7*, 2207−2217.

Dill, K. A., & Shortle, D. (1991) *Annu. Rev. Biochem. 60*, 795−825.

Duddeck, H. (1995) Günther Snatzke, *Liebigs Ann. 6*, *I*−*XIII*.

Fersht, A. R. (1993) *FEBS Lett. 325*, 5−16.

Fersht, A. R. (1995) *Curr. Opin. Struct. Biol. 5*, 79−84.

Frauenfelder, H., Sligar, S. G., & Wolynes, P. G. (1991) *Science 254*, 1598−1603.

Freund, S. M. V., Wong, K. B., & Fersht, A. R. (1996) *Proc. Natl. Acad. Sci. U.S.A. 93*, 10600−10603.

Hartley, R. W. (1988) *J. Mol. Biol. 202*, 913−915.

Holtzer, M. E., & Holtzer, A. (1992) *Biopolymers 32*, 1589−1591.

Jasanoff, A., & Fersht, A. R. (1994) *Biochemistry 33*, 2129−2135.

Jiang, M., Nölting, B., Stayton, P. S., & Sligar, S. G. (1996) *Langmuir 12*, 1278−1283.

Jung, C., Ristau, O., Schulze, H., & Sligar, S. G. (1996) *Eur. J. Biochem. 235*, 660−669.

Kalnin, N. N., & Kuwajima, K. (1995) *Proteins: Struct., Funct., Genet. 23*, 163−176.

Konno, T., Kataoka, M., Kamatari, Y., Kanaori, K., Nosaka, A., & Akasaka, K. (1995) *J. Mol. Biol. 251*, 95−103.

Kraulis, P. (1991) *J. Appl. Crystallogr. 24*, 946−950.

Kuwajima, K., Yamaya, H., & Sugai, S (1996) *J. Mol. Biol. 264*, 806−822.

Lubienski, M. J., Bycroft, M., Freund, S. M. V., & Fersht, A. R. (1994) *Biochemistry 33*, 8866−8877.

Makhatadze, G. I., & Privalov, P. L. (1993) *J. Mol. Biol. 232*, 639−659.

Neira, J. L., & Fersht, A. R. (1996) *Folding Des. 1*, 231−241.

Neri, D., Billeter, M., Wider, G., & Wüthrich, K. (1992) *Science 257*, 1559−1563.

Nölting, B., Golbik, R., & Fersht, A. R. (1995) *Proc. Natl. Acad. Sci. U.S.A. 92*, 10668−10672.

Nölting, B., Golbik, R., Neira, J. L., Soler-Gonzalez, A. S., Schreiber, G., & Fersht, A. R. (1997) *Proc. Natl. Acad. Sci. U.S.A. 94*, 826−830.

Parsegian, V. A., Rand, R. P., Fuller, N. L., & Rau, D. C. (1986) *Methods Enzymol. 127*, 400−416.

Perrett, S., Clarke, J., Hounslow, A. M., & Fersht, A. R. (1995) *Biochemistry 34*, 9288−9298.

Pfeil, W. (1988) *Biochemical Thermodynamics* (Jones, M. N., Ed.) pp 53−99, Elsevier, Amsterdam.

Pfeil, W., Nölting, B., & Jung, C. (1993) *Biochemistry 32*, 8856−8862.

Privalov, P. L. (1990) *Crit. Rev. Biochem. Mol. Biol. 25*, 281−305.

Privalov, P. L., & Makhatadze, G. I. (1993) *J. Mol. Biol. 232*, 660−679.

Schreiber, G., & Fersht, A. R. (1993) *Biochemistry 32*, 11195−11203.

Serrano, L. (1995) *J. Mol. Biol. 254*, 322−333.

Serrano, L., Horovitz, A., Avron, B., Bycroft, M., & Fersht, A. R. (1990) *Biochemistry 29*, 9343−9352.

Smith, L. J., Bolin, K. A., Schwalbe, H., MacArthur, M. W., Thornton, J. M., & Dobson, C. M. (1996) *J. Mol. Biol. 255*, 494−506.

Snatzke, G. (1994) in *Circular Dichroism* (Nakanishi, K., Berova, N., & Woody, R. W., Eds.) pp 1−38, VCH, New York, Weinheim, and Cambridge.

Su, Z. D., Arooz, M. T., Chen, H. M., Gross, C. J., & Tsong, T. Y. (1996) *Proc. Natl. Acad. Sci. U.S.A. 93*, 2539−2544.

Tanford, C. (1970) *Adv. Protein Chem. 24*, 1−95.

Tiffany, M. L., & Krimm, S. (1968) *Biopolymers 6*, 1767−1770.

Tiffany, M. L., & Krimm, S. (1969) *Biopolymers 8*, 347−359.

Tiffany, M. L., & Krimm, S. (1972) *Biopolymers 11*, 2309−2316.

Vuilleumier, S., Sancho, J., Loewenthal, R., & Fersht, A. R. (1993) *Biochemistry 32*, 10303−10313.

Wolynes, P. G., Onuchic, J. N., & Thirumalai, D. (1995) *Science 267*, 1619−1620.

Wolynes, P. G., Luthey-Schulten, Z., & Onuchic, J. N. (1996) *Chem. Biol. 3*, 425−432.

Wong, K. B., Freund, S. M. V., & Fersht, A. R. (1996) *J. Mol. Biol. 259*, 805−818.

Woody, R. W. (1978) *Biopolymers 17*, 1451−1467.

Woody, R. W. (1994) in *Circular Dichroism* (Nakanishi, K., Berova, N., & Woody, R. W., Eds.) pp 473−496, VCH, New York, Weinheim, and Cambridge.

BI962879U